Hydrogen Storage in Aluminum Hydride

Kazutaka Ikeda[1], Masaharu Menjo[1], Hai-Wen Li[1], Shunsuke Muto[2], Kazuyoshi Tatsumi[2], Kunihiko Hashi[3], Hideaki Itoh[3], Toshiki Kabutomori[4] and Shin-ichi Orimo[1]

[1]Institute for Materials Research, Tohoku University, Sendai 980-8577, Japan
[2]Department of Materials, Physics and Energy Engineering, Nagoya University, Nagoya 464-8603, Japan
[3]Muroran Research Laboratory, The Japan Steel Works, Ltd., Muroran 051-8505, Japan
[4]Research and Development Headquarters, The Japan Steel Works, Ltd., Tokyo 141-0032, Japan

Introduction

Aluminum trihydride (AlH_3, alane) is one of the potential candidates for hydrogen storage materials because of high gravimetric and volumetric hydrogen densities (10 mass% and 149 kgH_2/m^3, respectively) and a simple hydrogen desorption reaction ($AlH_3 \rightarrow Al + 3/2H_2$) at 370–470 K [1–4]. Among the variations of its crystalline structure [5–9], α-AlH_3 is the most stable, in which the enthalpy change of the hydrogen desorption reaction is in the range of –5.7 to –7.6 $kJ/molH_2$ [3, 10, 11]. This range indicates that the equilibrium hydrogen pressure of α-AlH_3 is around 1 GPa at 298 K [12]. A surface layer that is apparently composed of oxides is present on AlH_3 particles, which prevents the occurrence of the hydrogen desorption reaction of 'AlH_3' to Al at room temperature [4, 10, 11, 13]. It is of great importance to precisely study the nanostructures of the surface layer and the inside of the AlH_3 particles using microscope techniques [14, 15]. In this study, therefore, we performed nano-characterization of AlH_3 during the hydrogen desorption reaction by *in situ* microscopic observations combined with thermal and surface analyses.

Experimental

AlH_3 particles were prepared by the chemical reaction between $LiAlH_4$ and $AlCl_3$ in ether solution [3–5, 16, 17]; the particles were then examined by thermogravimetry analysis (TG, heating rate of 1 K/min under He) and powder X-ray diffraction measurement (XRD, Cu Kα radiation). The particles were dispersed on a carbon tape and microgrid mesh for *in situ* scanning electron microscopy (SEM, JEOL JSM6009, 3 kV) and transmission electron microscopy (TEM, JEOL JEM2100 with a Gatan ES500W Erlangshen CCD high-speed camera, 100 kV) observations, respectively. The TEM observations were performed under an electron flux of approximately 2×10^5 electrons/nm^2s for avoiding a damage of the particles by electron irradiation. A pellet of the particles was prepared for X-ray photoelectron spectroscopy (XPS, VG EscaLab spectrometer with SPECS PHOIBOS 100 analyzer, Mg Kα radiation, base pressure better than 10^{-9} mbar).

Results and Discussion

Fig. 1 shows the TG profile and SEM images during the hydrogen desorption reaction of the AlH_3 particles. The TG profile shows that the hydrogen desorption reaction starts at around 370 K and the amount of desorbed hydrogen is 9.6 ± 0.2 mass% (corresponding to 96% of the ideal amount in AlH_3, 10.1 mass%). From the XRD profiles shown in Fig. 2, we can also confirm the existence of the single phase of α-AlH_3 with a molecular volume of 33.4 $Å^3/\alpha$-AlH_3 and metallic Al with a molecular volume of 16.6 $Å^3$/Al before and after the hydrogen desorption reaction, respectively. The two-fold shrinkage in molecular volume from α-AlH_3 to metallic Al was highly expected to cause a change

in the morphologies of the primary particles. The SEM images, however, indicate that the morphologies of the particles with sizes of 100 nm–1 μm do not change at all during the hydrogen desorption reaction, as also shown in Fig. 1(a)–(c).

A TEM image of the primary AlH_3 particles before the hydrogen desorption reaction is shown in Fig. 3(a) [4, 15], and the particles are found to have sizes of around 100–200 nm. The electron diffraction patterns suggested that the particles before the hydrogen desorption reaction are single crystals of α-AlH_3 [4, 15]. The particles are covered by a surface layer (probably composed of oxides, described later) with a thickness of less than 5 nm.

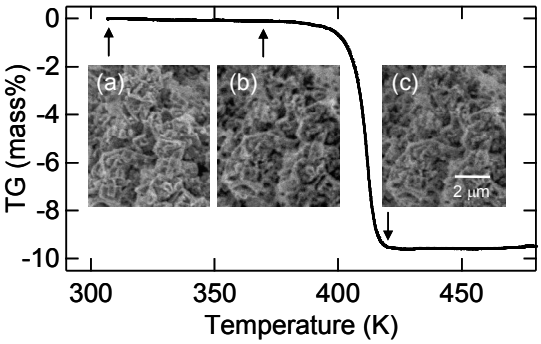

Fig. 1 Thermogravimetry (TG) profile of the AlH_3 particles. Insets show *in situ* SEM images; (a) before the hydrogen desorption reaction and during the reaction at (b) 370 K and (c) 420 K [4].

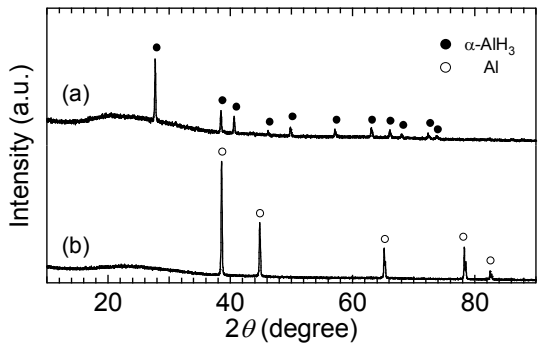

Fig. 2 Powder XRD profiles of the AlH_3 particles (a) before and (b) after the hydrogen desorption reactions [4].

Furthermore, the TEM images taken during the hydrogen desorption reaction (heating achieved by electron irradiation) are shown in Fig. 3(b) and (c). Clearly, nanoscale (~1 nm) precipitations can be observed inside the primary particles of size 100–200 nm; then, these precipitations exhibit a continuous grain-growth (20–50 nm). Simultaneously, the 'boundary space' in the primary particles increases because of the shrinkage in the molecular volume from α-AlH_3 to metallic Al, as described above. The electron diffraction pattern indicated the existence of polycrystalline metallic Al after the hydrogen desorption reaction [4, 15]; it may be noted that the polycrystals were formed from a single crystal of AlH_3 during the hydrogen desorption reaction. On the surface layer, neither the formation of cracks nor a change in thickness was observed during the hydrogen desorption reaction.

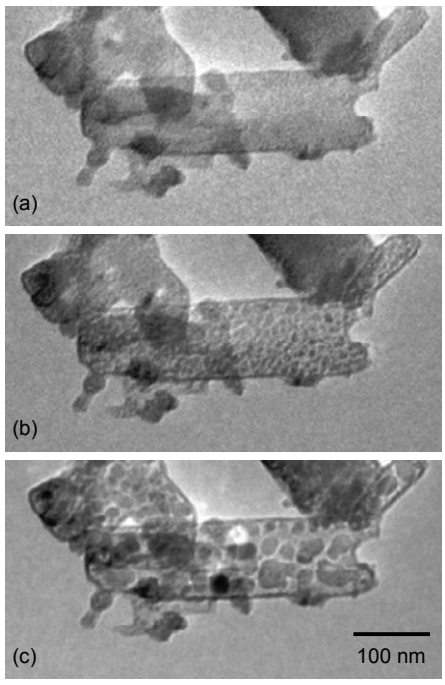

Fig. 3 TEM images of the primary AlH_3 particles (a) before, (b) during and (c) after the hydrogen desorption reaction [4, 15].

TEM observation before and after the thermal desorption reaction without electron irradiation were also carried out [15]. The morphology of the

final state is very similar to that produced by electron irradiation: metallic Al nanoscale particles were formed with their external shape almost unchanged because of the surface protecting layers.
It was, therefore, found that the surface morphology of the primary AlH_3 particles was not affected by the hydrogen desorption reaction; however the nanostructure inside the particles was found to change drastically by the precipitations and their continuous grain-growth of the metallic Al.
XPS profile of the primary AlH_3 particles before the hydrogen desorption reaction revealed O and Al [4]. In addition, EELS results confirmed that the surface layer covering the AlH_3 particles was thin amorphous alumina with a thickness of 3–5 nm [15]. As described in the introduction, the surface layer on the primary AlH_3 particles should play a dominant role against the occurrence of the hydrogen desorption reaction (thereby retaining the 'AlH_3' structure inside the particles) at room temperature. Further, hydrogen desorption evaluations of AlH_3 filled in small-scale hydrogen storage tank are currently in progress.

Conclusions

We attempted to elucidate the changes of the primary AlH_3 particles with the single phase of α-AlH_3 during the hydrogen desorption reaction. The particles with sizes of 100 nm–1 μm appear to be covered by an oxide layer with a thickness of less than 5 nm before the hydrogen desorption reaction. The morphology of the particles covered by the surface layer does not change during the hydrogen desorption reaction because there is neither an observable formation of cracks nor a change in the thickness of the surface layer during the reaction. On the other hand, both the precipitation/grain-growth of the polycrystalline metallic Al with sizes of 1–50 nm and an increase in the 'boundary space' were clearly observed inside the particles.

Acknowledgments

Synthesis and XPS measurements of the sample were done in collaboration with Dr. C. M. Jensen at University of Hawaii and Mr. S. Kato, Drs. M. Bielmann and A Züttel at EMPA. The authors thank Dr. Y. Nakamori for valuable discussions and Ms. H. Ohmiya for technical support. This work was supported in part by the seeds innovation project, the Japan Science and Technology Agency (JST); the Global COE Program 'Materials Integration, Tohoku University'; the inter-university cooperative research program of the Advanced Research Centre of Metallic Glasses, Institute for Materials Research, Tohoku University; Grants-in-Aid for Scientific Research KAKENHI (21760547) and Priority Areas (#474) 'Atomic Scale Modification' from MEXT, Japan. One of the authors (KI) is grateful to the Yazaki Memorial Foundation for Science and Technology.

References

1. Sandrock G., Reilly J., Graetz J., Zhou W.M., Johnson J. and Wegrzyn J. Accelerated thermal decomposition of AlH_3 for hydrogen-fueled vehicles. *Appl. Phys. A*, **80** (2005) 687–690.
2. Graetz J. and Reilly J. Decomposition Kinetics of the AlH_3 Polymorphs. *J. Phys. Chem. B*, **109** (2005) 22181– 22185.
3. Orimo S., Nakamori Y., Kato T., Brown C. and Jensen C.M. Intrinsic and mechanically modified thermal stabilities of α-, β- and γ-aluminum trihydrides AlH_3. *Appl. Phys. A*, **83** (2006) 5–8.
4. Ikeda K., Muto S., Tatsumi K., Menjo M., Kato S., Bielmann M., Züttel A., Jensen C.M. and Orimo S. Dehydriding reaction of AlH_3: *in situ* microscopic observations combined with thermal and surface analyses. *Nanotechnology*, **20** (2009) 204004-1–4.
5. Brower F.M., Matzek N.E., Reigler P.F., Rinn H.W., Roberts C.B., Schmidt D.L., Snover J.A. and Terada K. Preparation and Properties of Aluminum Hydride. *J. Am. Chem. Soc.*, **98** (1976) 2450–2453.

6. Brinks H.W., Istad-Lem A. and Hauback B.C. Mechanochemical Synthesis and Crystal Structure of α'-AlD_3 and α-AlD_3. *J. Phys. Chem. B*, **110** (2006) 25833–25837.
7. Brinks H.W., Langley W., Jensen C.M., Graetz J., Reilly J.J. and Hauback B.C. Synthesis and crystal structure of β-AlD_3. *J. Alloys Compd.*, **433** (2007) 180–183.
8. Yartys V.A., Denys R.V., Maehlen J.P., Frommen C., Fichtner M., Bulychev B.M. and Emerich H. Double-Bridge Bonding of Aluminium and Hydrogen in the Crystal Structure of γ-AlH_3. *Inorg. Chem.*, **46** (2007) 1051–1055.
9. Brinks H.W., Brown C., Jensen C.M., Graetz J., Reilly J.J. and Hauback B.C. The crystal structure of γ-AlD_3. *J. Alloys Compd.*, **441** (2007) 364–367.
10. Sinke G.C., Walker L.C., Oetting F.L. and Stull D.R. Thermodynamic Properties of Aluminum Hydride. *J. Chem. Phys.*, **47** (1967) 2759–2761.
11. Graetz J. and Reilly J.J. Thermodynamics of the α, β and γ polymorphs of AlH_3. *J. Alloys Compd.*, **424** (2006) 262–265.
12. Saitoh H., Machida A., Katayama Y. and Aoki K. Formation and decomposition of AlH_3 in the aluminum-hydrogen system. *Appl. Phys. Lett.*, **93** (2008) 151918-1–3.
13. Sandrock G., Reilly J., Graetz J., Zhoub W.M., Johnson J. and Wegrzyn J. Alkali metal hydride doping of α-AlH_3 for enhanced H_2 desorption kinetics. *J. Alloys Compd.*, **421** (2006) 185–189.
14. Beattie S.D., Humphries T., Weaver L. and McGrady G.S. Temporal and spatial imaging of hydrogen storage materials: watching solvent and hydrogen desorption from aluminium hydride by transmission electron microscopy. *Chem. Commun.*, (2009) 4448– 4450.
15. Muto S., Tatsumi K., Ikeda K. and Orimo S. Dehydriding process of α-AlH_3 observed by transmission electron microscopy and electron energy-loss spectroscopy. *J. Appl. Phys.*, in press.
16. Claudy P., Bonnetot B. and Letoffe J.M. Preparation and Physicochemical Properties of Aluminum-Hydride. *J. Therm. Anal.*, **15** (1979) 129–139.
17. Kato T., Nakamori Y., Orimo S., Brown C. and Jensen C.M. Thermal properties of AlH_3-etherate and its desolvation reaction into AlH_3. *J. Alloys Compd.*, **446–447** (2007) 276–279.